

Structural change from doping the gold cluster

Yiji Tang · Shu-guang Wang · Jia Li

Received: 25 April 2010 / Accepted: 25 June 2010 / Published online: 9 July 2010
© Springer-Verlag 2010

Abstract Doping gold clusters with a transition metal ($M@Au_n$) causes structural change. To determine the mechanism by which these changes occur, the central gold atom of Au_5 was doped with its same row transition metals Pt, Ir, Os, Re, and W. Based on theoretical calculations, a similar trend was found in other gold clusters.

Keywords Contract · Dope · Gold cluster · Structural change · Transition metal

Introduction

Clusters have recently been heatedly discussed among scientists [1, 2]. These materials constitute a bridge between small molecules and bulk solids, and are expected to have higher chemical reactivity [3]. Many theoretical studies have discussed the different types of transition metal clusters [4–6]. The gold nano-cluster has been proven to be a new class of such materials, and many scientists have studied it for its special characteristics [7–9]. Recently, gold-based bimetallic clusters have also caught increased attention [10–12]. Doping gold clusters with transition metals has been actively pursued in an attempt to tailor their structural, electronic, magnetic, and chemical properties for potential application [13]. Transition metal atoms doped into a small gold cluster ($M@Au_n$) can strongly change the properties of the cluster; such clusters, including those doped with Ag, Cu, and Pt [14–17], for example, have been widely studied. To the best of the authors' knowledge,

however, no theoretical study yet exists about how replacing one atom of a gold cluster with a third row transition metal can influence its structure.

This paper discusses the structural changes caused by the replacement of one atom in a gold cluster using theoretical calculations. To determine the mechanism by which these changes occur, the third row transition metals W, Re, Os, Ir, and Pt, all of which are adjacent to Au in the periodic table, were selected as doping atoms. Observations obtained were analyzed and extended to develop such a mechanism. Finally, expected structural changes were proven from further calculations.

Theoretical calculations

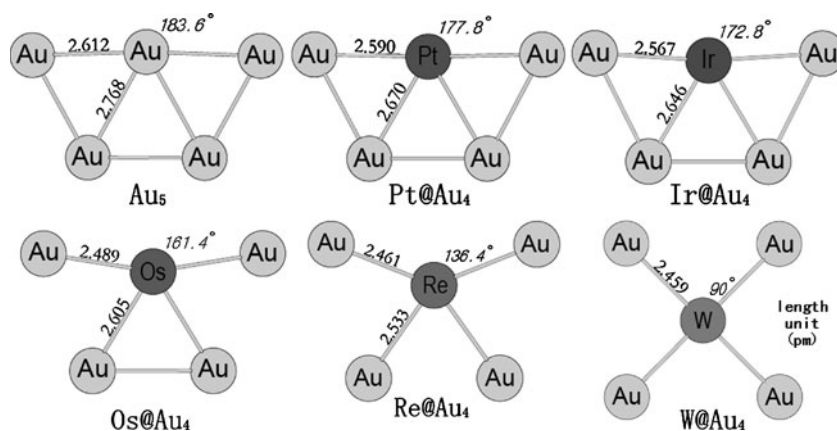
The system under analysis is made purely from transition metals. Density functional theory (DFT) calculations have been performed to assist in the characterization of the various intermediate species and to facilitate an understanding of the dynamic behavior of the system. All calculations in this work were carried out based on the density functional theory (DFT), as it has been shown to yield reliable results in calculations for transition-metal complexes [18].

Calculations were performed using the Gaussian03 program [19]. Two different DFT exchange-correlation potentials were used: (1) the local exchange functional ($X\alpha$) [20, 21], and (2) the non-local gradient-corrected exchange-correlation functional, Perdew-Wang 1991 (PW91) [22]. The former includes local spin density approximations (LSDA) while the latter includes components of the generalized gradient approximations (GGA) [23].

The structure was optimized at the Xalpha/lanl2dz level, as Wang's study has shown that the $X\alpha$ method works well with transition metals, especially gold cluster systems [24].

Y. Tang (✉) · S.-g. Wang · J. Li
School of Chemistry and Chemical Technology,
Shanghai Jiao Tong University,
Shanghai 200240, China
e-mail: tyj@sytu.edu.cn

Fig. 1 Structures of $M^i@Au_4$ ($M = Au, Pt, Ir, Os, Re, W$) (Length unit: Å)



Structure-optimization is generally considered to be insensitive to its basic sets, thus lanl2dz, the basis set that includes the Los Alamos effective core potential plus double zeta [25], was selected.

Energy was calculated at the pw91pw91/sdd level

Result and discussion

Third row transition metals Au, Pt, Ir, Os, Re, and W, all of which are adjoined in the period table and have a delicate relation, were doped one-by-one into the gold cluster ($M^i@Au_n$, i represents the atomic number) and caused dramatic structural changes to the gold cluster. The effects of replacing the central atom of the pentagon-shaped Au_5 are interesting to study because the central atom and its four side atoms constitute an open geometry that easily shows structural changes. The structure of $M^i@Au_4$ ($M^i = Au, Pt, Ir, Os, Re, W$) was calculated at the XAlpha/lanl2dz level, replaced the $M^{i+1}@Au_n$ cluster with the atom M^i (adjoined to M^{i+1} in the periodic table), and then optimized its structure (Fig. 1). The cluster contracted at the center atom, and this contraction increased as the replacement atom moved from $Au \rightarrow W$. Bond lengths shortened and cluster concaves where replaced. The figure changes from a pentagon into a square.

Generally, the contraction may be explained by the difference in atomic radii as we move from $Au \rightarrow W$. The atomic radius is half of the M-M distance. Clusters constitute the material between small molecules and bulk

Table 1 The metallic and covalent radii of the transition metal elements Au, Pt, Ir, Os, Re, and W

Transition metal element:	Au	Pt	Ir	Os	Re	W
Metallic radii/Å:	1.442	1.387	1.357	1.353	1.375	1.408
Covalent radii/Å:	1.44	1.28	1.37	1.28	1.59	1.46

solids, so studying their metallic and covalent radii is advisable. Different sets of atomic radii are available in literature [26–29], the text selected the study by Suresh and Koga [29] and are listed in Table 1. While analyzing the metallic and covalent radii of the series elements $Au \rightarrow W$, both featured complex changes, some of which did not meet the monotonic trend of the contractions observed. Thus, these contractions occurred should be explored.

The apparent difference between the elements from $Au \rightarrow W$ is the number of valence electrons of each atom. From $Au \rightarrow W$, the number of valence electrons decreases one by one from $5d^{10}6s^1$ to $5d^46s^2$. To determine how this decrease affects the structure of the cluster, the MO of these clusters was calculated at the pw91pw91/sdd level and their valence shells studied (Fig. 2), because molecular orbitals are approximated as a linear combination of atomic orbitals.

When the valence shells of two adjoining clusters, Au_4M^i and Au_4M^{i-1} , were compared (Fig. 2), their energy levels were not significantly different. Most evident was the reduction of the electron occupied by the HOMO of Au_4M^i .

Orbital representations of the HOMOs involved are shown in Fig. 3. From the initial $M^i@Au_4$ structure, HOMO is seen to be the anti-bonding orbital, and the main nodal plane of the wave function is between the central

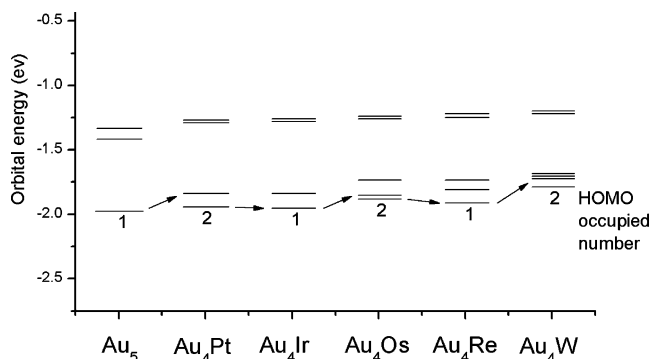


Fig. 2 The valence shell's condition of $M^i@Au_4$ ($M^i = Au, Pt, Ir, Os, Re, W$)

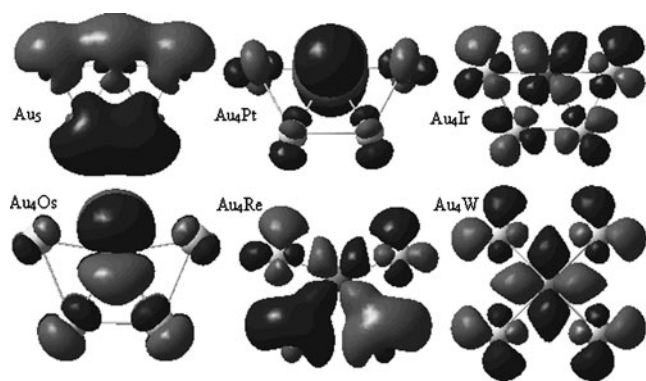


Fig. 3 HOMOs of the wave functions of $M^i@Au_4$ ($M^i = Au, Pt, Ir, Os, Re, W$)

atom M^i and the four Au atoms to its side. Following the definition of bond order (θ), the difference in the occupancy of the bonding (f_0) and antibonding (f_1) states [30]:

$$\theta = (f_0 - f_1)/2 \quad (1)$$

The reduction of occupancy in the anti-bonding orbital (f_1) causes an increase in the bond order (f_0). As a result, the bond strengthens and shortens [31, 32]. Atom replacement therefore makes the cluster Au_4M^i contract in the direction of the nodal plane. In the previous case, contraction moves toward the central atom in the $M^i@Au_4$ cluster.

As to the molecular orbital Ψ , the wave functions are expressed as linear combinations of atomic orbital (φ):

$$\Psi_i = \sum_j c_{ij} \varphi_j \quad (2)$$

In this paper, among the Ψ_i , those which have the highest energy are generally considered to be anti-bonds, because after the linear combination of AO (φ), the MO (Ψ) of anti-bonding obtains an increase in energy opposite to that of bonding [33].

Among transition metals, the electronic structure of Au has some special features, including the fact that it only has 1 electron (a half orbital) in its valence shell ($5d^{10}6s^1$), leaving the shell incompletely filled. Since the number of orbitals and electrons in the valence shell keep the electronic balance before and after linear combinations, gold or even gold-based clusters ($M^i@Au_n$) have an abundance of electrons in their valence shells and several MOs with their highest energy levels unoccupied [34].

Table 2 The atomic radius R_{CCR} of Au, Pt, Ir, Os, Re, and W

Transition metal element:	Au	Pt	Ir	Os	Re	W
$R_{CCR}/\text{\AA}$:	1.74	1.77	1.80	1.85	1.88	1.93

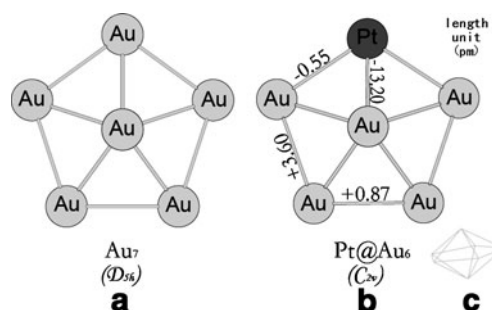


Fig. 4 (a) The pentagon-bipyramid Au_7 from the vertical angle perspective. The five gold atoms on the equator level are equal to one another. (b) Replacing one Pt atom in the gold cluster on the equator level brings significant changes in comparison with the previous structure (length unit: pm). (c) The structure of (b) from a three-dimensional perspective. (Because of the symmetry, only a few bonding changes can be displayed)

With regard to gold clusters, considering that the 6 s and 5d orbital of Au have a close level spacing in energy, even hybridization may often be seen in their molecule [35]. Thus, the MO in (2) consists of different s and d orbital components and shows little difference in energy. Therefore, in the gold cluster system, these orbits with high energy in the valence shell (including HOMO) prefer to be anti-bonds. Replacement from $Au \rightarrow W$ will thus cause a decrease in HOMO occupancy, which, in turn, will increase bond order and cause contraction.

Another possible reason for the contraction in bond lengths observed have to do with the increasing atomic orbital radii of the atoms from $Au \rightarrow W$, as expected from the vertical and horizontal trend in atomic size in the periodic table [36]. The orbital radius is a set of theoretical atomic radii that corresponds to the principle maximum in the radial distribution function [28]. The data of atomic orbital radius selected, which was determined from the minimal-basis-set SCF functions studied by Clementi, Raimondi, and Reinhardt, called R_{CCR} [37], are listed in Table 2. Th0065 larger orbital radii, caused by the replacement from $Au \rightarrow W$, increase the overlap integral (not the overlap population) of the valence:

$$S = \int \Psi_A \Psi_B dv \quad (3)$$

The bond strengthens as its length shortens because the bonding effect is proportional to the S integral. As a result, contraction occurs where an atom in the cluster is replaced.

As for why the Au-Au bonds disappear (approximately 3.5 Å) in the flat $W@Au_4$, it should be the valence shell of Au is $5d^{10}6s^1$, which means it only lacks one electron in the valence shell, but that of W is $5d^5$ which means it has much greater ability to have bonding with other atoms. While bonding with W, the Au becomes full in the valence shell, so it is meaningless for the Au atoms to bond with each other. Therefore the Au-Au bonds almost disappear in Au_4W .

Fig. 5 (a) The structural change obtained by doping Pt to a side atom of Au₆ (b) The structural change obtained by doping Pt to the central atom of Au₉ (c) The structural change obtained by doping Pt to the top atom of Au₁₀ (Because of the symmetry, only a few bonding changes can be displayed) (length unit: pm)

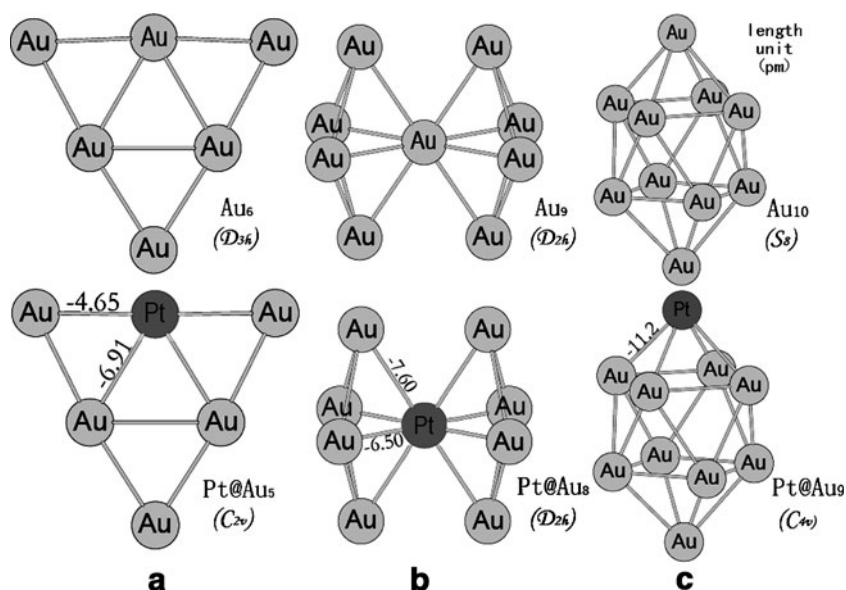


Figure 4 shows the structural changes that occur when a Pt atom is doped into the equator surface of the pentagon-bipyramid Au₇. Initially, the five atoms at the equator level are symmetrical from the perspective of the vertical angle. Figure 4 shows that contraction of the bond lengths occurs where replacement takes place. The Pt-Au bonds shortened, while some Au-Au bonds lengthened due to tension effects.

These explanations bear important considerations for gold cluster systems. Replacing atoms in a gold cluster system seems to cause contractions in bond length.

Figure 5 shows the structural effects of replacing an atom in the gold cluster system of Au_n with the Pt atom at various locations in the cluster, thus producing Pt@Au_{n-1}. Doping Pt to a side atom of the D_{3h}-Au₆ cluster results in contractions to the bond lengths of this side. Replacing the central atom of C_{2v}-Au₉ causes contractions to the bond lengths at the center of the cluster. In the same manner, replacing the top atom of S₈-Au₁₀ with Pt shows contractions to the bond lengths at this location. Contraction obviously occurs where an atom in the gold cluster is replaced.

Conclusions

Third row transition metals Au, Pt, Ir, Os, Re, and W were doped into gold clusters (Mⁱ@Au_n) to study the structural changes these metals bring about to the cluster. These metals caused contractions in bond lengths at the Mⁱ atom. This may be explained by the effect of the differences in valence electron number, which was found to cause increasing bonding order (from Au → W) in the system. The findings may also be attributed to the increasing atomic radii (R_{CCR}) of the metals, which strengthens the bonding

effect from Au → W in Mⁱ@Au_n. The replacement of several atoms in the gold cluster clearly demonstrated these structural changes.

Acknowledgments We thank our friends Xin Zheng, Yalei Ji, Zhicong Xie, Zhe Chen, Chao Xiao, Yuanpei Cao, Yang Fei, Jie Chen and the referees for many illuminating comments.

References

1. Heer WA (1993) The physics of simple metal clusters: experimental aspects and simple models. *Rev Mod Phys* 65:611–676
2. Kelly KL, Coronado E, Zhao LL, Schatz GC (2003) The optical properties of metal nanoparticles: The influence of size, shape, and dielectric environment. *J Phys Chem B* 107:668–677
3. Bell AT (2003) The Impact of Nanoscience on Heterogeneous Catalysis. *Science* 299:1688–1691
4. Baletto F, Ferrando R, Fortunelli A, Montalenti F, Mottet C (2002) Crossover among structural motifs in transition and noble-metal clusters. *J Chem Phys* 116:3856–3863
5. Morse MD (1986) Clusters of transition-metal atoms. *Chem Rev* 86:1049–1109
6. Lombardi JR, Davis B (2002) Periodic Properties of Force Constants of Small Transition-Metal and Lanthanide Clusters. *Chem Rev* 102:2431–2460
7. Deka A, Deka RC (2008) Structural and electronic properties of stable Au_n (n=2–13) clusters: A density functional study. *J Mol Struct THEOCHEM* 870:83–93
8. Hammer B, Nørskov JK (1995) Why gold is the noblest of all the metals. *Nature* 376:238–240
9. Valden M, Lai X, Goodman DW (1998) Onset of Catalytic Activity of Gold Clusters on Titania with the Appearance of Nonmetallic Properties. *Science* 281:1647–1650
10. Pykkö P, Runeberg N (2002) Icosahedral WAu₁₂: A predicted closed-shell species, stabilized by aurophilic attraction and relativity and in accord with the 18-electron rule. *Angew Chem* 41:2174–2176
11. Zhai HJ, Li J, Wang LS (2004) Icosahedral gold cage clusters: M@Au₁₂ - (M = V, Nb, and Ta). *J Chem Phys* 121:8369–8374

12. Neukermans S, Janssens E, Tanaka H, Silverans RE, Lievens P (2003) Element- and size-dependent electron delocalization in AuNX + clusters (X = Sc, Ti, V, Cr, Mn, Fe, Co, Ni). *Phys Rev Lett* 90:033401/1-033401/4
13. Li X, Kiran B, Cui LF, Wang LS (2005) Magnetic properties in transition-metal-doped gold clusters: M@Au 6 (M = Ti, V, Cr). *Phys Rev Lett* 95:1–4
14. Tian WQ, Ge M, Gu F, Yamada T, Aoki Y (2006) Binary clusters AuPt and Au6Pt: Structure and reactivity within density functional theory. *J Phys Chem A* 110:6285–6293
15. Jian JG, Ji XY, Dong D (2006) First principle calculation on AuPt₂ (n=1–4) clusters. *J Mol Struct Theochem* 764:117–121
16. Pyykkö P, Runeberg N (2002) Icosahedral WAu₁₂: A predicted closed-shell species, stabilized by aurophilic attraction and relativity and in accord with the 18-electron rule. *Angew Chem* 41:2174–2176
17. Guo JJ, Yang JX, Die D (2007) First principle calculation on AuAg₂ (n=1–4) clusters. *Commun Theor Phys* 48:348–352
18. Niu S, Hall MB (2000) Theoretical Studies on Reactions of Transition-Metal Complexes. *Chem Rev* 100:353–406
19. Frisch MJ, Trucks GW, Schlegel HB, Scuseria GE, Robb MA, Cheeseman JR, Montgomery JA, Vreven T Jr, Kudin KN, Burant JC, Millam JM, Iyengar SS, Tomasi J, Barone V, Mennucci B, Cossi M, Scalmani G, Rega N, Petersson GA, Nakatsuji H, Hada M, Ehara M, Toyota K, Fukuda R, Hasegawa J, Ishida M, Nakajima T, Honda Y, Kitao O, Nakai H, Klene M, Li X, Knox JE, Hratchian HP, Cross JB, Adamo C, Jaramillo J, Gomperts R, Stratmann RE, Yazyev O, Austin AJ, Cammi R, Pomelli C, Ochterski JW, Ayala PY, Morokuma K, Voth GA, Salvador P, Dannenberg JJ, Zakrzewski VG, Dapprich S, Daniels AD, Strain MC, Farkas O, Malick DK, Rabuck AD, Raghavachari K, Foresman JB, Ortiz JV, Cui Q, Baboul AG, Clifford S, Cioslowski J, Stefanov BB, Liu G, Liashenko A, Piskorz P, Komaromi I, Martin RL, Fox DJ, Keith T, Al-Laham MA, Peng CY, Nanayakkara A, Challacombe M, Gill PMW, Johnson B, Chen W, Wong MW, Gonzalez C, Pople JA (2004) Gaussian 03, Revision C.02. Gaussian Inc, Wallingford, CT
20. Slater JC (1951) A Simplification of the Hartree-Fock Method. *Phys Rev* 81:385–390
21. Schwarz K (1972) Optimization of the Statistical Exchange Parameter α for the Free Atoms H through Nb. *Phys Rev B* 5:2466–2468
22. Perdew JP, Chevary JA, Vosko SH, Jackson KA, Pederson MR, Singh DJ, Fiolhais C (1992) Atoms, molecules, solids, and surfaces: Applications of the generalized gradient approximation for exchange and correlation. *Phys Rev B* 46:6671–6687
23. Long J, Qiu YX, Chen XY, Wang SG (2008) Stable geometric and electronic structures of gold-coated nanoparticles M@Au₁₂ (M= 5d transition metals, from Hf to Hg): Ik or Ok? *J Phys Chem C* 112:12646–12652
24. Qiu YX, Wang SW, Schwarz WHE (2004) Gold coated M@Au₁₂ nano-particles: Assessment of different quantum chemical density functional approaches. *Chem Phys Lett* 397:374–378
25. Hay PJ, Wadt WR (1985) Ab initio effective core potentials for molecular calculations. Potentials for K to Au including the outermost core orbitals. *J Chem Phys* 82:299–310
26. Cordero B, Gómez V, Platero-Prats AE, Revés M, Echeverría J, Cremades E, Barragán F, Alvarez S (2008) Covalent radii revisited. *Dalton Trans* 2008:2832–2838
27. Gibbs GV, Tamada O, Boisen MB (1997) Atomic and ionic radii: A comparison with radii derived from electron density distributions. *J R Phys Chem Miner* 24:432–439
28. Ghosh DC, Biswas R, Chakraborty T, Islam N, Rajak SK (2008) The wave mechanical evaluation of the absolute radii of atoms. *J Mol Struct Theochem* 865:60–67
29. Suresh CH, Koga N (2001) A consistent approach toward atomic radii. *J Phys Chem A* 105:5940–5944
30. Finnis MW (2007) Bond-order potentials through the ages. *Prog Mater Sci* 52:133–153
31. Chang TC (1997) Lewis bond order for some controversial canonical molecular orbitals. *J Mol Struct Theochem* 391:151–157
32. Cioslowski J, Mixon ST (1991) Covalent bond orders in the topological theory of atoms in molecules. *J Am Chem Soc* 113:4142–4145
33. Magnasco V (2005) On the principle of maximum overlap in molecular orbital theory. *Chem Phys Lett* 407:213–216
34. Roothaan CCJ (1951) New Developments in Molecular Orbital Theory. *Rev Mod Phys* 23:69–89
35. Brocksch HJ, Bennemann KH (1985) Tight-binding study of the structural stability of the (110) surface of the 5d-transition metals Ir, Pt and Au. *Surf Sci* 161:321–341
36. Ghosh DC, Biswas R (2002) Theoretical calculation of absolute radii of atoms and ions. Part 1. Theatomic radii. *Int J Mol Sci* 3:87–113
37. Clementi E, Raimondi DL, Reinhardt WP (1967) Atomic screening constants from SCF functions. II. Atoms with 37 to 86 electrons. *J Chem Phys* 47:1300–1307